

---

# Continually Learning Structured Visual Representations via Network Refinement with Rerelation

---

Zeki Doruk Erden<sup>1</sup> Boi Faltings<sup>1</sup>

## Abstract

Current machine learning paradigm relies on continuous representations like neural networks, which iteratively adjust parameters to approximate outcomes rather than directly learning the structure of problem. This spreads information across the network, causing issues like information loss and incomprehensibility. Building on prior work in environment dynamics modeling, we propose a method that learns visual space in a structured, continual manner. Our approach refines networks to capture the core structure of objects while representing significant subvariants in structure efficiently. We demonstrate this with 2D shape detection, showing incremental learning on MNIST without overwriting knowledge and creating compact, comprehensible representations. These results offer a promising step toward a transparent, continually learning alternative to traditional neural networks for visual processing.

## 1. Introduction

Modern machine learning relies on neural networks to model complex systems, achieving remarkable success in areas like image recognition and NLP (Khan et al., 2021; Zhao et al., 2023), yet as these problems are solved, crucial shortcomings at their core start to gain attention (Clune, 2019; Zador, 2019; Marcus, 2018; LeCun, 2022). Importantly, they struggle with continual learning—the ability to learn new tasks without forgetting previous ones, as essential for open-ended learning, reflecting real-world dynamics. This limitation necessitates frequent, resource-intensive re-training, making scalability impractical. Furthermore, the overparameterized, unstructured design of neural networks has prioritized performance over comprehensibility, limiting trust, control, and adaptability in complex environments. The lack of comprehensibility in AI is a critical concern

as systems grow more capable. Neural networks’ opaque nature makes their internal workings hard to understand, refine, or integrate with structured systems. This opacity hinders human validation, corrective adjustments, and the incorporation of explicit knowledge. Without these capabilities, using AI in critical decision-making poses risks absent in more transparent engineering domains.

An alternative exists: we can retain the power of advanced learning systems while prioritizing structure, transparency, and control by focusing research on these goals. This is essential for building adaptable, human-aligned systems suited for real-world complexities. Prior work (Erden & Faltings, 2024a; 2025b;a) has demonstrated the viability of frameworks that incorporate minimal, yet rich, representations of data to achieve continual learning and interoperability on simple environment dynamics modeling, offering a clear path toward systems that align more closely with human understanding. In this paper, we expand on these advancements by proposing a novel framework to apply these foundational ideas to the domain of observation spaces that can be represented as networks, in particular to visual information processing. Our approach refines these principles to create a continual and structured learning process for vision, emphasizing the capture of essential object structures while hierarchically organizing frequently observed subvariants. This method ensures that knowledge is continually learned without disrupting existing representations and creates compact, directly human-comprehensible representations. It further lays the groundwork for applying the broader framework from (Erden & Faltings, 2025a) to visual domains, supporting structured representations for modeling environment dynamics.

We demonstrate the potential of our approach with a proof-of-concept shape detection task on 2D objects. The model learns incrementally from the MNIST dataset, retaining knowledge while incorporating new information without task boundaries or replay, and generates structured, human-comprehensible representations. This showcases the potential of this type of approach as a transparent alternative to traditional neural networks, capable of learning continually by design, hence addressing key challenges in machine learning in general as well as for visual processing.

<sup>1</sup>Artificial Intelligence Laboratory, École Polytechnique Fédérale de Lausanne, Lausanne, Switzerland. Correspondence to: Zeki Doruk Erden <zeki.erden@epfl.ch>.

## 2. Related work

Two most important core limitations of current ML systems are the inability of continual learning and incomprehensibility of internal structure; problems often tackled in isolation (Kirkpatrick et al., 2017; Rusu et al., 2016; Jacobson et al., 2022; Hadsell et al., 2020; Zhuang et al., 2020; Xu et al., 2019). Solutions proposed for these problems often don’t fully resolve the fundamental limitations of NNs in this regard but aim to mitigate their effects.

Many continual learning methods rely on simplifying assumptions, such as externally defined task boundaries and task change information (Rusu et al., 2016; Jacobson et al., 2022), or storing and replaying past observations (Buzzega et al., 2020), which bias learning toward previous tasks without enabling true continual learning (Kirkpatrick et al., 2017). These issues also affect visual problems (Qu et al., 2021), where even state-of-the-art techniques depend on replay buffers (Galashov et al., 2023) or task boundaries (Wang et al., 2022). One exception is methods generating multiple experts and assigning tasks based on a generative model (Erden & Faltings, 2024b; Lee et al., 2020). While powerful, these methods still assume distinct tasks by decomposing the system into experts, relying on the assumption that bulk data is available for each expert’s generative model. This assumption holds in offline experimentation but not in continual learning, where data is distributed over time and not available in bulk. Thus, the continual learning problem shifts to the generative model for task identification rather than the entire system. Additionally, none of these methods address model comprehensibility alongside continual learning, which shares the same root cause.

Current approaches to making learned models comprehensible, categorized under Explainable AI methods (Xu et al., 2019; Kashefi et al., 2023) offer post-hoc explanations for neural network operations but fail to address the core incomprehensibility of their internal structures, leaving them hard to trustfully validate and engineer. Visual processing with neural networks faces the same issue (Kashefi et al., 2023). Moreover, comprehensibility is often treated separately from continual learning, rather than as a shared challenge. Studies that consider both tend to propose distinct mechanisms for each problem (Roy et al., 2022) or focus on specific explainability issues arising from certain continual learning methods (Rymarczyk et al., 2023; Cossu et al., 2024).

These limitations are inherent to neural networks and similar methods, and attempting to address them within the same paradigm either proves impossible or leads to excessive methodological complexity. Recent work has proposed *varsel mechanisms* (Erden & Faltings, 2025a;b), which learn via local variation and selection, mimicking biological adaptation (Marc, 2005; Gerhart & Kirschner, 2007). The method, Modelleyen (Erden & Faltings, 2024a; 2025a;b),

enables continual learning without task boundaries, task change information, or replay buffers, while also creating an inherently comprehensible structure by learning with minimal complexity at each level. This approach addresses both continual learning and explainability/comprehensibility by tackling their shared root cause: nonstructured representations.

## 3. Method

### 3.1. Background: Modelleyen and Varsel mechanisms

Previous studies ((Erden & Faltings, 2024a), (Erden & Faltings, 2025b), (Erden & Faltings, 2025a)) introduced *Modelleyen* as an example of proposed *varsel mechanisms*, which learn through component-level topological variation and selection to model external environments or tasks. This contrasts with methods like neural networks that rely on fine-tuning continuous parameters without explicitly learning network topology. Due to space constraints, we provide only a brief overview here; for full details, see (Erden & Faltings, 2024a; 2025b;a) and Section A.1 for the formal learning algorithm from these papers.

The learning core of the *varsel* network in *Modelleyen* consists of *conditioning (state) variables (CSVs)*, which, along with raw observations and target predictions, form the model’s building blocks, akin to neurons in neural networks. The method in (Erden & Faltings, 2024a; 2025a) exhaustively connects CSVs with other state variables (representing raw observations or their discrete activation dynamics) based on observed data at each time instant, then refines these connections with further observations (see Fig. 6 in Appendix). Higher-order CSVs are formed upstream (Fig. 7 in Appendix) to predict downstream CSV states when conflicts arise, enabling the representation of arbitrary logical functions. Theorem 1 in (Erden & Faltings, 2024a) proves a strong continual learning property: a CSV’s response to a past instance  $x_0$  remains consistent even after structural modifications from new instances  $x_i$ , provided no negative sources formation occurs in the meantime. Although system-wide performance retention is not guaranteed due to mechanisms like suppressive connections or component removals, this still ensures local information retention and consistency, providing a potent guarantee of knowledge preservation with system-wide reflections verified experimentally (Erden & Faltings, 2025a).

Previous work validated *Modelleyen* on low-dimensional finite state machines; yet highlighted the need for extensions to handle higher-dimensional and structured observation spaces, particularly for operating on networks rather than lists of state variables (Erden & Faltings, 2025a). Our method extends this approach, adapting *Modelleyen*’s principles to process visual observations, as detailed in the fol-

lowing subsections.

### 3.2. Continually learning structured visual representations

We aim to extend the framework from (Erden & Faltings, 2025a) to operate on *networks* as observations, rather than raw state variables. Networks can represent diverse domains, particularly spatial and temporal observations relevant to AI. Our focus is on vision, specifically 2D shape identification, though the approach is generalizable to any network-representable observation provided an appropriate representational conversion is used. The method is agnostic to how a 2D image is converted into a network. We detail our experimental feature representation in Section 3.3, but for this section, the reader can think about a generic concept of a visual feature that can refer to edges, colors, gradients, objects, or even raw pixels. We refer to this design as *Modelleyen with network refinement* (MNR for short).

#### 3.2.1. REPRESENTATIONAL BASIS

First, let’s define the basis for our representation of observations and input sources for conditioning state variables (CSVs) in this extension:

**Definition 3.1.** A *state network* (SN) is a directed graph  $(N, E)$ , where each node  $N$  has an associated *type*. A list of tuples of state networks and associated keys,  $P = [(k_0, SN_0), (k_1, SN_1), \dots]$  is called a *state polynetwork* (SPN).

Node types in state networks (SNs) represent distinct features (e.g., edges, corners, or objects in visual space), with nodes being observed instances of these features in the current observation (e.g., two edges with the same orientation or two instances of the same object are distinct nodes of the same type; see Figure 2a for an example). Edges ( $E$ ) represent relations between nodes, such as relative positions in visual inputs or succession in temporal domains. A state polynetwork (SPN) is a collection of distinct state networks with a designator key, enabling the definition of different feature and relation types. In visual space, this could include shape, color gradients, or abstract objects, as well as multi-dimensional relations (e.g., relative positioning). An example SPN is shown in Figure 3c (its means of construction from images is detailed in the next section).

SPNs will serve as input sources for CSVs in our model, replacing the sets of state variables in (Erden & Faltings, 2024a; 2025a). Learning the model involves constructing SPN structures that capture the desired information, bringing us to the question of how an SPN (representing a CSV’s input configuration) should be modified in response to new SPN observations.

#### 3.2.2. NETWORK REFINEMENT WITH RERELATION

Refinement, the core learning process in *Modelleyen* (Erden & Faltings, 2024a; 2025a), reduces two lists of state variables (sources for a CSV) to their intersection, retaining only the subset necessary to activate the CSV. An analogous operation is needed to identify the *shared part* of two or more state polynetworks (SPNs), forming the basis for the model-level learning flow (discussed in Sec. 3.2.3).

For that purpose, we make the following definition:

**Definition 3.2.** An SPN  $P_0 = [(k_0, SN_0^0), (k_1, SN_1^0), \dots, (k_N, SN_N^0)]$  is *satisfied* by another SPN  $P_1 = [(k_0, SN_0^1), (k_1, SN_1^1), \dots, (k_N, SN_N^1)]$  (with the same set of keys  $K = [k_0, k_1, \dots, k_N]$ ) given a potentially partial *assignment*  $f : V(P_0) \rightarrow V(P_1)$ , where  $N(P_i)$  is the set of all nodes across all state networks of  $P_i$ , if and only if the following conditions hold:

1. For  $\forall n_0 \in N(P_0)$ ,  $f(n_0)$  is defined (has a mapped node in  $N(P_1)$ ), and
2. For  $\forall e_0 = (n_0, n_1) \in E(SN_i^0)$  where  $E(SN_i^0)$  is the set of all edges in state network  $SN_i^0$  in  $P_0$ , there exists a path in  $SN_i^1$  from  $f(n_0)$  to  $f(n_1)$ .

Intuitively,  $P_0$  is satisfied by  $P_1$  under an assignment if every node in  $P_0$  has a corresponding target node in  $P_1$ , and every edge in  $P_0$  has a path in  $P_1$  connecting the assigned targets of its endpoints within the same SN. This ensures that all entities and relations in  $P_0$  are present in  $P_1$ , even if mediated by additional entities not in  $P_0$  (as paths, not direct edges, are required).

We can now redefine “finding the intersection” of two SPNs  $P_0$  and  $P_1$  as “minimally refining  $P_0$  to be satisfied by  $P_1$ .” This is achieved through *network refinement with rerelation*, where  $P_0$  (source) is refined by  $P_1$  (refiner). The process, detailed in Algorithm 1, relies on two subprocesses:

- *Refinement*: Nodes in  $P_0$  that are missing in  $P_1$ , and edges in SNs of  $P_0$  that don’t have a path between their endpoints in the corresponding SN of  $P_1$ , are removed.
- *Rerelation*: When an edge  $(n_0, n_1)$  is removed (including via node removal), a new edge  $(p_i, s_i)$  is created for  $\forall p_i \in P(n_0), s_i \in S(n_1)$ , where  $P(n)$  and  $S(n)$  are predecessors and successors of node  $n$  respectively. (Each edge formed by rerelation is checked for the same conditions of presence as existing ones.)

Figure 1 illustrates this process: the source SPN in 1a is refined by the refiner in 1b, resulting in the refined SPN in 1c. Paths like  $(A, D)$  or  $(A, C)$  are preserved despite differing intermediaries. Applying this process sequentially to a

---

**Algorithm 1** Network refinement with rerelation.

---

**Function-RefineBy**( $P_0, P_1, f$ )

**Parameters:**  $P_0$ , source SPN.  $P_1$ , refiner SPN.  $f$ , a partial assignment between nodes in  $P_0$  to nodes in  $P_1$ .

```

1: for  $SN_i^0 \in P_0$  do
2:   for  $n \in nodes(SN_i^0)$  do
3:     if  $f(n)$  not defined then
4:       for  $(n_0, n_1) \in edges(SN_i^0, n)$  do
5:         RemoveWithRerelation( $SN_i^0, n_0, n_1$ )
6:       end for
7:        $SN_i^0.RemoveNode(n)$ 
8:     end if
9:   end for
10:  for  $(n_0, n_1) \in edges(SN_i^0)$  do
11:    if  $path(f(n_0), f(n_1))$  not in  $SN_i^1$  then
12:      RemoveWithRerelation( $SN_i^0, n_0, n_1$ )
13:    end if
14:  end for
15: end for
    
```

**Function-RemoveWithRerelation**( $SN, n_0, n_1$ )

```

1: for  $(p, s) \in prod(P_{SN}(n_0), S_{SN}(n_1))$  do
2:    $SN.AddEdge(p, s)$ 
3: end for
4:  $SN.RemoveEdge(n_0, n_1)$ 
    
```

---

source SPN across multiple refiners results in a final SPN representing commonalities across all refiners, ensuring it is satisfied by each refiner retrospectively.<sup>1</sup>

**Statistical Refinement** Given the noisy experimental domain, we enhanced Algorithm 1 by incorporating node/edge observation statistics. Instead of removing a node/edge upon its first absence, we remove it only if the ratio of its absences exceeds a threshold  $T_{ref} \in (0, 1)$ . This prevents losing important features potentially missed due to noise or misassignment (see below). Being a more constrained removal condition, this maintains *Modelleyen*’s continual learning guarantees.

**Assignments** A key issue in extending the base *Modelleyen* framework to network refinement is finding a suitable (possibly partial) node mapping  $f : V(P_0) \rightarrow V(P_1)$  between two SPNs. The only constraint is that source nodes can only map to nodes of the same type (i.e., representing the same feature). However, multiple valid mappings may exist, resulting in different post-refinement structures (see Figure 2). To address this, we used the following approach: We

<sup>1</sup>The local continual learning guarantee in *Modelleyen* (Theorem 1 in (Erden & Faltings, 2024a; 2025a)) also applies to Algorithm 1, as nodes and paths in an SPN are analogous to state variables in the base version. Thus, the theorem’s proof holds for node and path removal, with edge refinement being more constrained than path refinement.

create a population of alternative assignments by pairing nodes from the source and refiner SPNs based on shared node types. While this works well with a small number of nodes per type, our feature representation (Section 3.3) often requires additional prioritization. To address this, we rank node pairs by their positional proximity in both SPNs, using the negative softmax of the distance between candidate pairs to probabilistically select the most suitable assignments. After generating the population, we calculate a *mismatch score* for each assignment, representing the total number of nodes and paths in the source SPN missing from the refiner SPN. The assignment with the lowest mismatch score—requiring the least refinement—is selected.

In our experiments, this assignment mechanism produced effective mappings (see Section 5). However, it is not flawless, and selecting the optimal assignment from the population remains the most computationally intensive step in our workflow. Further research could likely improve this process or even eliminate the need for such assignments altogether.

### 3.2.3. LEARNING FLOW

As in (Erden & Faltings, 2024a), our system design defines a *model* using *conditioning state variables (CSVs)*, which describe relationships between their *sources* (state polynetworks, or SPNs) and *targets* (other CSVs or specific target state variables). The learning flow largely follows Modelleyen’s approach (see (Erden & Faltings, 2025a) and Algorithms 2 & 3 in the Appendix for details), except for the following adjustments:

1. Unlike (Erden & Faltings, 2024a; 2025a), where upstream CSVs integrate with lower-level CSVs via an *and* condition, our implementation treats upstream CSVs as observed *subvariants* of their CSV targets, with source SPNs encompassing the source SPNs of them. This allows assignments from lower-order CSVs to propagate upstream, eliminating redundant assignments and simplifying the learning flow by avoiding the need for additional subnetwork definitions.
2. Unlike (Erden & Faltings, 2025a), which creates a common CSV for all targets in a step, we assume a single target per CSV and create separate CSVs (with identical sources) for each target. This change supports the upstream assignment propagation in previous point.
3. Instead of embedding negative (suppressing) sources within a CSV, we externalize them into separate CSVs. A negatively-conditioning CSV is formed when a state variable with an inactive state and no active negative conditioner is observed (with potentially multiple formed per target). We also redefine the *unconditionality* flag to deactivate upon the first observation of



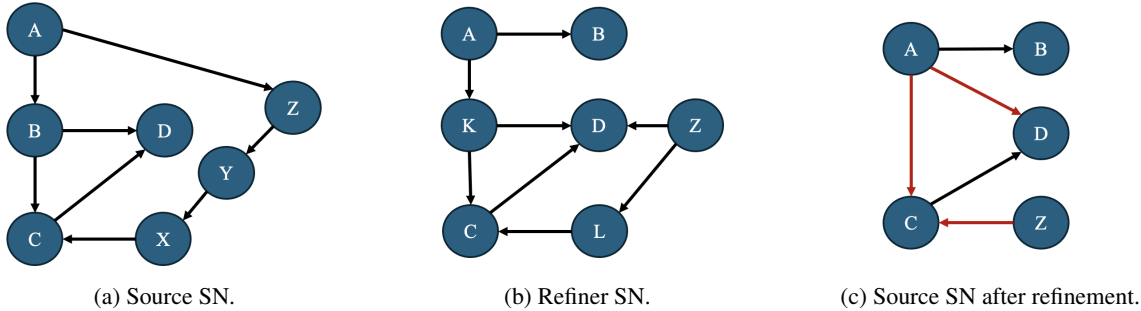


Figure 1. Illustration of network refinement with rerelation. In (c), highlighted edges are created through rerelation. Paths  $(A, D)$  and  $(A, C)$  exist in both networks but are mediated by different intermediaries (B and K respectively), leading to refined intermediaries and new edges. Similarly, path  $(Z, C)$ , mediated by  $(Y, X)$  in the source and  $(L)$  in the refiner, is refined. Edge  $(A, Z)$  is removed as it lacks a corresponding path in the refiner SPN. Edge  $(A, B)$  is preserved unchanged, as it appears in both networks, despite differing successors of B. (Node positions are illustrative and irrelevant to refinement.)

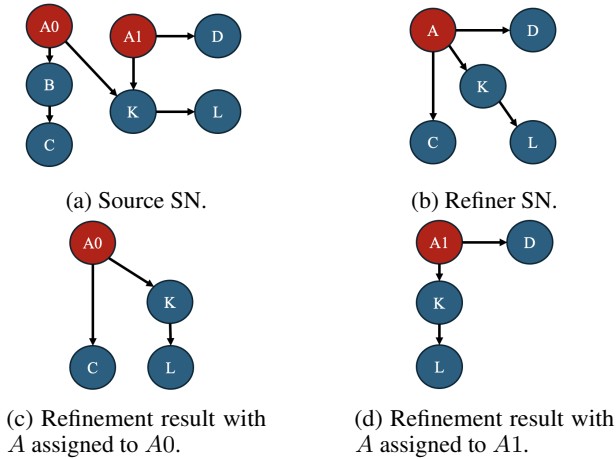


Figure 2. A node ( $A$ ) of a given type (red) in the refiner SPN can map to multiple nodes in the source network ( $A0$  or  $A1$ ), resulting in two post-refinement networks with no clear superior assignment.

an inactive state, allowing simultaneous positive and negative upstream conditioning.

- Instead of the complex  $NCC$  metric in (Erden & Faltings, 2025a), we filter insignificant conditioners by removing a conditioner  $C$  of target  $T$  if  $P(SS(C)|I(T)) < T_{sign}$ , where  $SS(C)$  and  $I(T)$  represent the satisfaction of  $C$ 's sources and the observation of  $T$ 's state, respectively.

The major changes, outlined in points 1 and 2, primarily affect CSV composition without altering the core learning flow or CSV state definitions. These changes were made for implementation simplicity and will be modified in future framework developments to include multiple targets and distinct upstream networks, improving representational efficiency (see Section 5).

Currently, the operational flow is computationally intensive, limiting simulations to shorter durations. At this stage, our focus is on designing and validating the learning flow rather than optimizing the algorithm or capping model complexity, though these aspects are briefly discussed in Section 6.

### 3.3. Feature representation for basic shape learning

*Modelleyen with network refinement* (MNR) is applicable to any observation space representable as networks. For our experiments, we focus on demonstrating the method in a basic visual processing domain: 2D shape identification in binary images, using MNIST as the test domain. This task is foundational in computer vision and has historically served as a starting point for approaches like neural networks (LeCun et al., 1998; Cortes, 1995). Below, we detail the feature representation (image-to-network conversion) used. We note that this is only demonstrative for the use of our approach in a simple context, but future work can extend it to other types, including 2D features like color gradients or 3D features with spatial positions, as the domain requires.

To ensure generality in shape detection and avoid overly hand-crafted features, we use *horizontal* ( $x$ ) and *vertical* ( $y$ ) *gradient orientation change points*. Our image processing flow involves: (1) converting a grayscale image to binary with a 50% threshold, (2) approximating contours as polygons using OpenCV's Ramer–Douglas–Peucker algorithm (OpenCV, 2025), yielding corners and oriented edges (CW for outer, CCW for inner contours) (Figure 3b), and (3) computing the sign of gradients at each corner in the  $x$  and  $y$  dimensions based on edge orientation (e.g., a rightward-facing edge has a negative  $x$ -axis gradient).

We build the final SPN using corners where gradient orientations change in the  $x$  or  $y$  axes. Traversing the contour in its connected direction (CW or CCW), we create a node for each corner if the gradient direction (positive or negative)

changes in either axis from the predecessor to the successor edge. The node type is defined by the change axis, direction, and corner convexity. For example, the top-right corner in Figure 3b represents a convex corner with a y-gradient change from positive to negative, resulting in a node of type "convex, +y to -y" (node  $cx\_ypos\_yneg\_0$  in Fig. 3c). This process defines the SPN's nodes.

Our SPN includes four types of SNs: *contour*, *inner*, *outer*, and *all*. *Contour* SNs represent connections along the contour, linking nodes as described earlier, with edges added between predecessors and successors of skipped corners. *Inner* and *outer* SNs connect nodes with straight lines that stay within the inner (pixel value 1) or outer (value 0) regions of the binary image. *All*-type SNs combine all connections, regardless of type, to persistently represent relative positional relationships even when their actual types can vary across images. Each network type has *horizontal* and *vertical* variants, where directed edges indicate positional relationships along the respective axis. For example, a directed edge  $(n_0, n_1)$  in *contour-horizontal* means  $n_0$  is to the left of  $n_1$ . See Fig. 3c for an example SPN.

*Limitations and possible extensions:* This representation is broadly applicable and domain-agnostic for 2D shape detection, relying on contours matching image gradients. However, it's mainly for demonstrating our design and has limitations, such as limited expressivity from not capturing all details of the shape but only those that represent gradient sign changes (e.g., only three of five corners are used in Fig. 3c). This affects final identification accuracy, making it fall short from a perfect performance as discussed in Section 5. A more complete approach would consider all gradient orientation changes, increasing complexity but also completeness. Likewise, it currently works for shape detection, but could be extended to other 2D features or 3D spaces with similar logic. Additionally, for learning with a vassel mechanism, shape detection might benefit from alternative representations like pixel-level processing, CNN filters, or frequency-based transformations, as discussed in the Conclusion. Finally, we note that multiple feature types can be used with SPN representation, either in separate networks or within the same network, capturing positional relations between features across domains. While we don't explore this here, it's an interesting direction for future work.

### 4. Experimental setup

We experiment on MNIST dataset, with the aim to (1) show continual learning performance of MNR, and contrast it with the learning progression of neural networks, and (2) investigate learned representations of classes by MNR for proper structure and comprehensibility.

Our MNR learning process involves randomly selecting  $N_C$

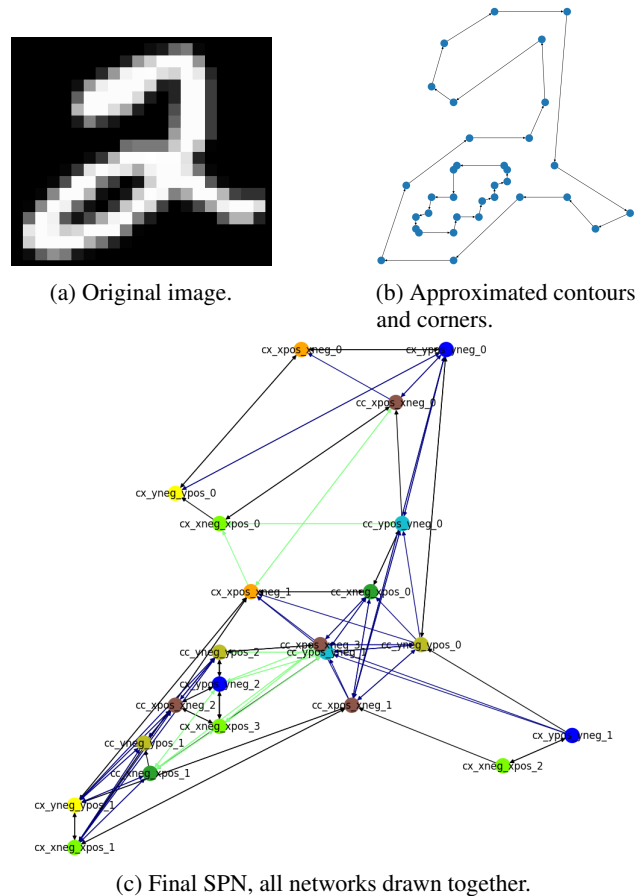
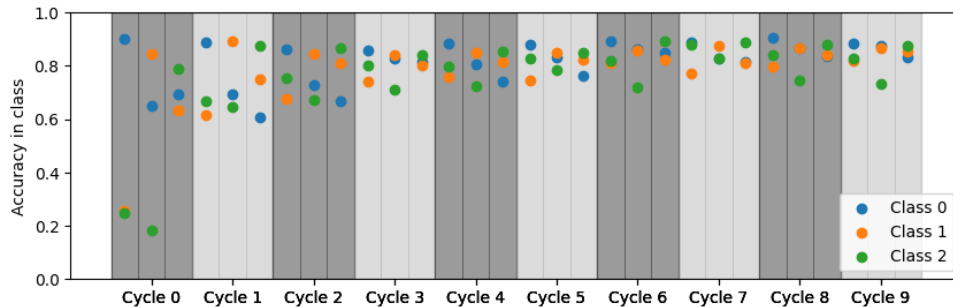
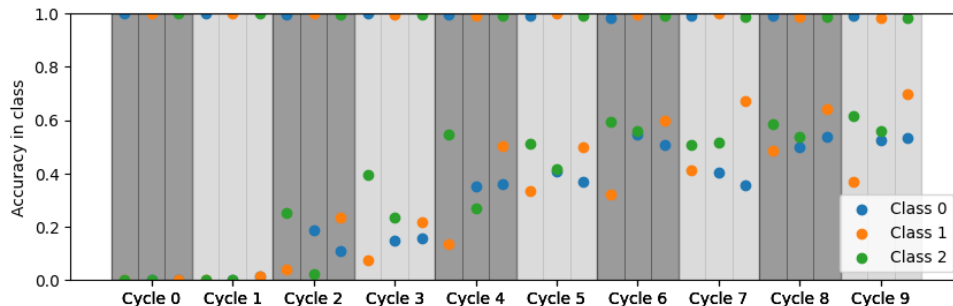


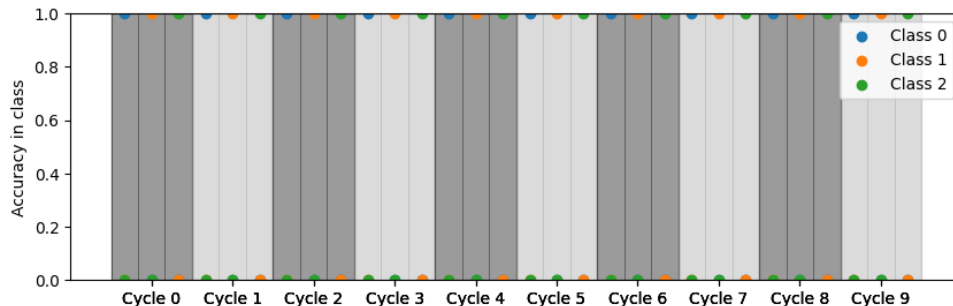
Figure 3. Example SPN construction from an image for 2D shape identification. In (c), blue, green, and black edges denote inner, outer, and contour connections, respectively. Nodes, colored by type, represent gradient change points (e.g., "cc\_xneg\_xpos\_1" indicates a concave corner with x-gradient shifting from (-) to (+)).



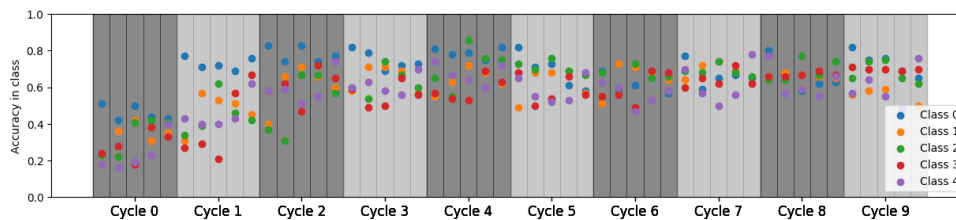
(a) MNR,  $N_C = 3$ .



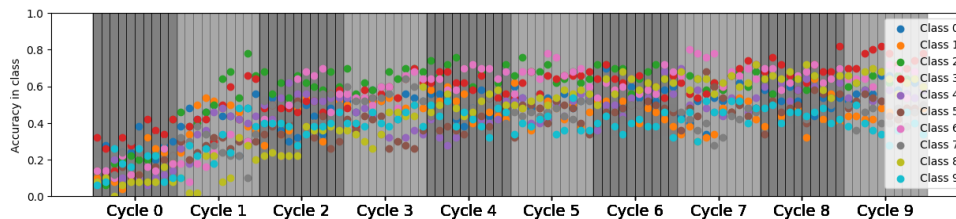
(b) Fully connected neural network,  $N_C = 3$ .



(c) Convolutional neural network,  $N_C = 3$ .



(d) MNR,  $N_C = 5$ .



(e) MNR,  $N_C = 10$ .

Figure 4. Learning performance of MNR, fully connected, and convolutional neural networks on  $N_C$ -class incremental learning over 10 cycles. Accuracies reflect correct classification ratios for each class. Shaded areas denote cycles, and vertical lines separate iterations within cycles. Results are averaged over 10 (a-c) and 5 (d-e) runs. Note that class indices  $i$  are randomly chosen at the start of each run and do not necessarily correspond to digit  $i$ .

classes from the 10 available at the start of each trial. In one *cycle*, the system is exposed to  $N_{sample}$  samples from each class sequentially, with one exposure and learning step per sample (no reexposure, as repeated steps have no effect in MNR). Processing samples from one class constitutes an *iteration*. Neural networks follow the same flow, trained on one sample per step until convergence or max epochs. Performance is evaluated via per-class accuracy after each iteration ( $N_C$  evaluations per cycle). We train for 10 such cycles, simulating a general and realistic continual flow on information with the requirement of ongoing learning without any constraining assumptions. Examples for model comprehensibility demonstrations are drawn from these experiments. We run our experiments on MNR with  $N_C = 3, 5$  and 10, and with  $N_C = 3$  on NNs for comparison of behavior. Reported results are averages of 10 and 5 runs for  $N_C = 3$  and 5 respectively. Further details, including choice of parameters and computation of predictions in MNR, can be found on Appendix A.3.

We do not provide a experimental comparison with existing continual learning methods since, as discussed in Section 2, every proposed method we are aware of operates with significant constraining assumptions, notably either replay buffers or clear task boundaries, which MNR does not have and was designed specifically to not have. It is known that existing methods can show near-perfect retention of information using while operating under these limiting assumptions (Erden & Faltings, 2024b), hence any partial comparison such as taking them as an upper baseline wouldn't be informative.

## 5. Results and discussion

### 5.1. Continual learning

Figure 4 shows learning progression of MNR for  $N_C = 3, 4$ , and 5 classes; as well as that of the neural network variants for  $N_C = 3$  for comparison.

MNR's final performance, as expected, does not achieve perfect identification, with accuracies of 85%, 60% and 50% for  $N_C = 3, 5$  and 10 respectively after 10 cycles. This stems primarily from limitations of feature representation (Section 3.3) and while it suggests the need for improvement with better representations (see Conclusions), it is not our main focus here. To validate continual learning of our design, we focus on MNR's high retention of learned information, as shown in Figures 4a, 4d, and 4e. Performance on class  $i$  remains stable in later iterations ( $j > i$ ) of the same cycle, with early accuracy persisting throughout. This contrasts sharply with neural networks: a fully connected NN (Fig. 4b) loses all information on class  $j > i$  in early cycles, and even after 10 cycles, it fails to retain a stable representation, showing  $> 50\%$  accuracy loss. A convolutional NN performs worse, losing all information repeatedly.

Continual learning is most critical in early cycles (first 3-4), as in the long run, with increasing number of cycles, the problem is equivalent to stochastic gradient descent with a slow timescale, reducing the problem to statistical learning with data abundance where NNs already excel. MNR's retention of performance is consistent across tests with 5 and 10 classes as well, albeit with lower baseline accuracies.

We note that in MNR, as in Modelleyen (Erden & Faltings, 2025a), even when there are small performance fluctuations, it is by design not due to direct destruction of existing information (unless a conditioner is removed for cumulative insignificance) but stems from over-refinement or negative conditioning.

We briefly note the factors limiting performance compared to the perfect detection achieved by neural networks. First, the representation used lacks full expressivity, capturing only gradient change points rather than all shape features (see Section 3.3). Second, the current statistical refinement approach retains some features not present in every sample of a class, yet SPN satisfaction (Definition 3.2) requires precise matches. This leads to missed instances, especially outliers. This is rather straightforward to offset by allowing soft satisfaction of SPNs (Definition 3.2). These limitations were not the focus of this work, which prioritized validating the learning flow with a demonstrative representation, and will be addressed in future research.

### 5.2. Comprehensibility of learned representations

Figure 5 illustrates samples of the learned SPNs, ranging from general representations at lower depths (near the target variable) to more specific ones at higher depths capturing rarer subvariants. These representations are visually intuitive, effectively depicting the digits, their features, and interrelations. For instance, most contours of digit "2" are preserved in Fig. 5a, though features like holes at the lower-left turning point (common in some samples like that in Fig. 3) are omitted, while persistent features, such as the vertical gradient change ("*cx\_yneg\_ypos\_1*"), are retained. Similarly, digit "5" in Fig. 5b retains key features, including vertical gradient changes on the right and horizontal changes at the top and bottom, along with correct positional relations. While general contours of "5" are refined at depth 0, they are preserved at the more specific subvariants upstream, like in Fig. 5c which provide more details. Some additional examples are also provided in Figure 8 in Appendix.

## 6. Conclusions, Limitations and Future Work

This work extended prior research on structured representations for continual learning, focusing on higher-dimensional observation spaces that can be represented as networks, particularly in visual domains, without constraining assump-



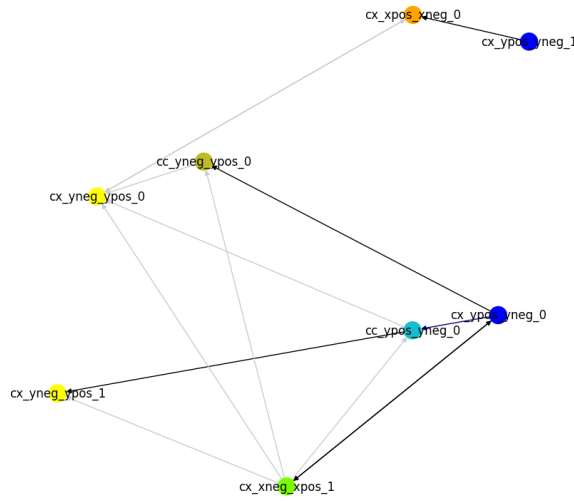
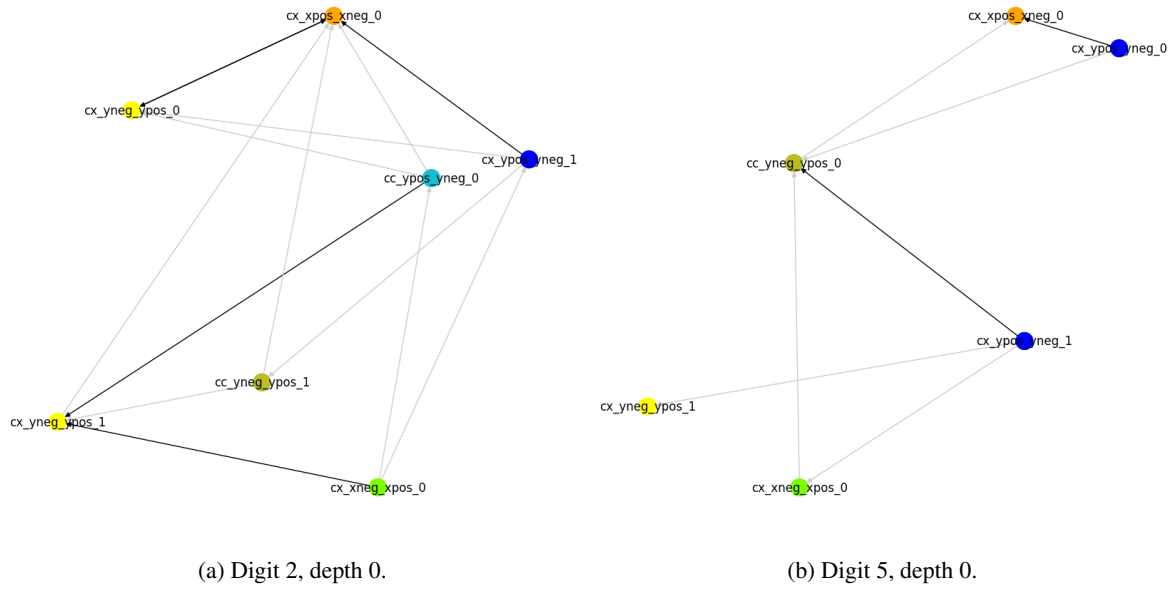


Figure 5. Sample source SPNs learned by the system, shown with all SNs combined. Blue, black, and gray edges represent inner, contour, and all-type connections, respectively. Depths indicate conditioning distance from the target variable (number of CSVs in the conditioning path). Node positions reflect the average of all observed positions during the CSV’s lifetime. Additional examples are in Fig. 8 in A.2.

tions and ensuring model comprehensibility. To that end, we introduced the mechanism of learning via network refinement with rerelation in Modelleyen learning flow, applied it to 2D shape identification with a proposed feature representation, and demonstrated its functionality. While final performance didn't match NNs due to limitations in feature expressivity, our core design aims were validated by (1) achieving continual learning without constraining assumptions, retaining past knowledge consistently, and (2) producing representations easily comprehensible by humans. This method also lays the groundwork for the integration of a means to process structured visual spaces into the broader framework of modeling environment dynamics and deliberative behavior in (Erden & Faltings, 2025a).

The current feature representation is a simple, demonstrative approach based on gradient sign changes, specifically designed for 2D shape detection. While it captures many key features, it is expressively limited, as evidenced by the performance shortfalls. Future work should focus on enhancing this expressivity. One option is to refine the edge-gradient-based method, which theoretically contains all the necessary shape information and hence remains a strong candidate. Alternatively, well-established computer vision methods, such as SIFT (Lindeberg, 2012) or pretrained neural networks like visual foundation models ((Oquab et al., 2023)), could be used for feature representation while retaining the MNR flow for high-level learning. Another promising direction is the use of frequency components (Xu et al., 2020), which are especially well-suited to this learning framework. Pixel-level detection, similar to NNs, could also be considered if scalability challenges are addressed, though this might unnecessarily complicate the model and reduce its interpretability. Intermediate representations, such as fixed-size filters similar to those used in CNNs, are another possibility. These approaches could improve the model's performance and extend its applicability beyond 2D shape identification.

The current implementation of our method is computationally demanding due to redundancies in modelling included for methodological simplicity, as optimization was not our focus at this stage. Upstream CSVs are represented as larger networks encompassing their downstream targets instead of distinct, integrated subnetworks, and each CSV is restricted to a single output, preventing shared conditioning sources. These design choices, while easy to modify, inflate computational demands. Furthermore, current learning flow processes multiple intersecting upstream paths simultaneously, which could be streamlined by handling only the "best-matching" path at each step, narrowing the upstream network being processed. Although the model in Modelleyen can grow as large as needed, operations should ideally involve only a small set of CSVs, with their combined source SPNs no more complex than the SPN representing given observation. This would cap per-step computation

complexity to the size of the observation space, and our aim is to realize this degree of computational efficiency.

A natural long-term extension of this work is processing more complex visual spaces, which would require hierarchical representations. While moderately simple structures (e.g., eyes or noses) can be plausibly learned using an approach similar to what is described in this work, more complex entities (e.g. whole faces) or multi-object scenes demand hierarchical organization of components. Our method is well-suited for such structured spaces, as they often involve fewer alternative assignments (e.g., unique objects). Future work will explore such extensions into hierarchical representations, and means for their unsupervised construction through the progression of learning.

## References

- Buzzega, P., Boschini, M., Porrello, A., Abati, D., and Calderara, S. Dark experience for general continual learning: a strong, simple baseline. *Advances in neural information processing systems*, 33:15920–15930, 2020.
- Clune, J. Ai-gas: Ai-generating algorithms, an alternate paradigm for producing general artificial intelligence. *arXiv preprint arXiv:1905.10985*, 2019.
- Cortes, C. Support-vector networks. *Machine Learning*, 1995.
- Cossu, A., Spinnato, F., Guidotti, R., and Bacciu, D. Drifting explanations in continual learning. *Neurocomputing*, pp. 127960, 2024.
- Erden, Z. D. and Faltings, B. Modelleyen: Continual learning and planning via structured modelling of environment dynamics. In Itthipuripat, S., Ascoli, G., Li, A., Pat, N., and Kuai, H. (eds.), *Brain Informatics: 17th International Conference, BI 2024, Bangkok, Thailand, December 13–15, 2024, Proceedings*. Springer Singapore, 2024a.
- Erden, Z. D. and Faltings, B. Directed structural adaptation to overcome statistical conflicts and enable continual learning. In *AAAI 2024, Deployable AI Workshop*, 2024b.
- Erden, Z. D. and Faltings, B. Agential ai for integrated continual learning, deliberative behavior, and comprehensible models, 2025a. URL <https://arxiv.org/abs/2501.16922>.
- Erden, Z. D. and Faltings, B. Agential ai for integrated continual learning, deliberative behavior, and comprehensible models (extended abstract). In *Proceedings of 24th International Conference on Autonomous Agents and Multiagent Systems (AAMAS)*, May 2025b. To appear.

- Galashov, A., Mitrovic, J., Tirumala, D., Teh, Y. W., Nguyen, T., Chaudhry, A., and Pascanu, R. Continually learning representations at scale. In *Conference on Lifelong Learning Agents*, pp. 534–547. PMLR, 2023.
- Gerhart, J. and Kirschner, M. The theory of facilitated variation. *Proceedings of the National Academy of Sciences*, 104(suppl\_1):8582–8589, 2007.
- Hadsell, R., Rao, D., Rusu, A. A., and Pascanu, R. Embracing change: Continual learning in deep neural networks. *Trends in cognitive sciences*, 24(12):1028–1040, 2020.
- Jacobson, M. J., Wright, C. Q., Jiang, N., Rodriguez-Rivera, G., and Xue, Y. Task detection in continual learning via familiarity autoencoders. In *2022 IEEE International Conference on Systems, Man, and Cybernetics (SMC)*, pp. 1–8. IEEE, 2022.
- Kashefi, R., Barekattain, L., Sabokrou, M., and Aghaeipoor, F. Explainability of vision transformers: A comprehensive review and new perspectives. *arXiv preprint arXiv:2311.06786*, 2023.
- Khan, A. A., Laghari, A. A., and Awan, S. A. Machine learning in computer vision: a review. *EAI Endorsed Transactions on Scalable Information Systems*, 8(32):e4–e4, 2021.
- Kirkpatrick, J., Pascanu, R., Rabinowitz, N., Veness, J., Desjardins, G., Rusu, A. A., Milan, K., Quan, J., Ramalho, T., Grabska-Barwinska, A., et al. Overcoming catastrophic forgetting in neural networks. *Proceedings of the national academy of sciences*, 114(13):3521–3526, 2017.
- LeCun, Y. A path towards autonomous machine intelligence version 0.9. 2, 2022-06-27. *Open Review*, 62(1), 2022.
- LeCun, Y., Bottou, L., Bengio, Y., and Haffner, P. Gradient-based learning applied to document recognition. *Proceedings of the IEEE*, 86(11):2278–2324, 1998.
- Lee, S., Ha, J., Zhang, D., and Kim, G. A neural dirichlet process mixture model for task-free continual learning. *arXiv preprint arXiv:2001.00689*, 2020.
- Lindeberg, T. Scale invariant feature transform. 2012.
- Marc, K. *The plausibility of life*. Yale University Press, 2005.
- Marcus, G. Deep learning: A critical appraisal. *arXiv preprint arXiv:1801.00631*, 2018.
- OpenCV. Shape analysis - opencv documentation, 2025. URL [https://docs.opencv.org/4.x/d3/dc0/group\\_\\_imgproc\\_\\_shape.html#ga0012a5fd8a70b8a9970165d98722b4c](https://docs.opencv.org/4.x/d3/dc0/group__imgproc__shape.html#ga0012a5fd8a70b8a9970165d98722b4c). Accessed: 2025-01-29.
- Oquab, M., Darcet, T., Moutakanni, T., Vo, H., Szafraniec, M., Khalidov, V., Fernandez, P., Haziza, D., Massa, F., El-Nouby, A., et al. Dinov2: Learning robust visual features without supervision. *arXiv preprint arXiv:2304.07193*, 2023.
- Qu, H., Rahmani, H., Xu, L., Williams, B., and Liu, J. Recent advances of continual learning in computer vision: An overview. *arXiv preprint arXiv:2109.11369*, 2021.
- Roy, H., Bhattacharjee, D., and Krejcar, O. Interpretable local frequency binary pattern (lfrbp) based joint continual learning network for heterogeneous face recognition. *IEEE Transactions on Information Forensics and Security*, 17:2125–2136, 2022.
- Rusu, A. A., Rabinowitz, N. C., Desjardins, G., Soyer, H., Kirkpatrick, J., Kavukcuoglu, K., Pascanu, R., and Hadsell, R. Progressive neural networks. *arXiv preprint arXiv:1606.04671*, 2016.
- Rymarczyk, D., van de Weijer, J., Zieliński, B., and Twardowski, B. Icicle: Interpretable class incremental continual learning. In *Proceedings of the IEEE/CVF International Conference on Computer Vision*, pp. 1887–1898, 2023.
- Wang, Z., Liu, L., Duan, Y., Kong, Y., and Tao, D. Continual learning with lifelong vision transformer. In *Proceedings of the IEEE/CVF Conference on Computer Vision and Pattern Recognition*, pp. 171–181, 2022.
- Xu, F., Uszkoreit, H., Du, Y., Fan, W., Zhao, D., and Zhu, J. Explainable ai: A brief survey on history, research areas, approaches and challenges. In *Natural Language Processing and Chinese Computing: 8th CCF International Conference, NLPCC 2019, Dunhuang, China, October 9–14, 2019, Proceedings, Part II 8*, pp. 563–574. Springer, 2019.
- Xu, K., Qin, M., Sun, F., Wang, Y., Chen, Y.-K., and Ren, F. Learning in the frequency domain. In *Proceedings of the IEEE/CVF conference on computer vision and pattern recognition*, pp. 1740–1749, 2020.
- Zador, A. M. A critique of pure learning and what artificial neural networks can learn from animal brains. *Nature communications*, 10(1):3770, 2019.
- Zhao, W. X., Zhou, K., Li, J., Tang, T., Wang, X., Hou, Y., Min, Y., Zhang, B., Zhang, J., Dong, Z., et al. A survey of large language models. *arXiv preprint arXiv:2303.18223*, 2023.
- Zhuang, F., Qi, Z., Duan, K., Xi, D., Zhu, Y., Zhu, H., Xiong, H., and He, Q. A comprehensive survey on transfer learning. *Proceedings of the IEEE*, 109(1):43–76, 2020.

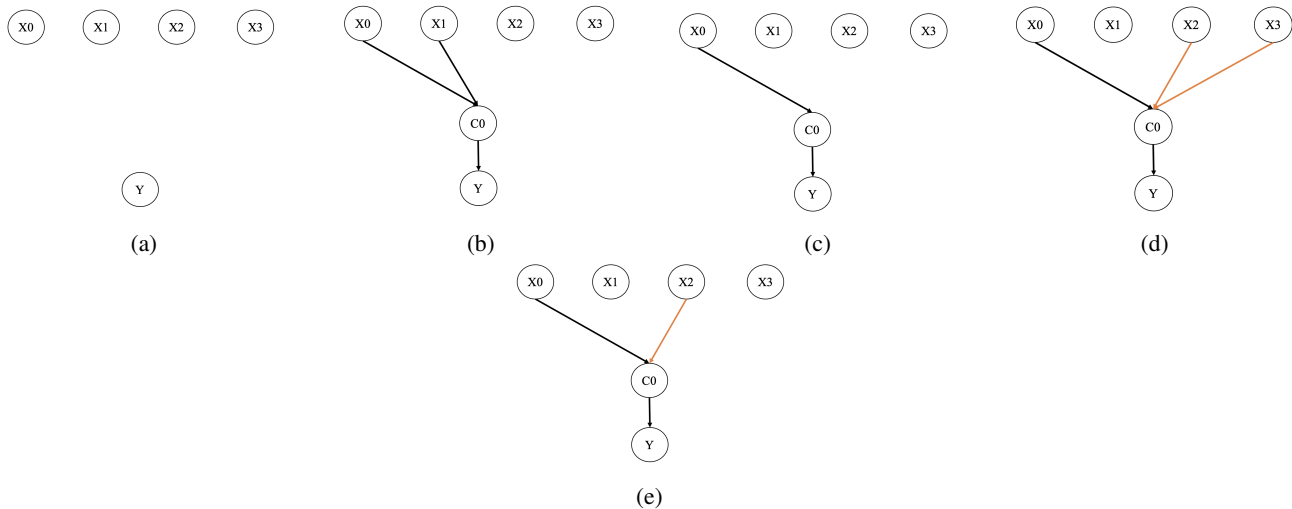


Figure 6. From (Erden & Faltings, 2025a). Sample formation of a CSV in a continual manner. The relationship to be modelled is  $Y = X_0 \text{ and } !X_2$  (“!” denotes “not”). Black and orange arrows represent positive and negative sources for CSV  $C_0$  respectively.  $X_i$  can be interpreted either as single or grouped SVs. (a) Initial state with no relation formed between  $X_0 - 3$  and  $Y$ . (b)  $X_0, X_1 \rightarrow Y$  observed. Positive connections hypothesizing both  $X_0$  &  $X_1$  are required for  $Y$  are formed. (c)  $X_0 \rightarrow Y$  is observed.  $X_1$  is deduced unnecessary for  $Y$ . (d)  $X_0, X_2, X_3 \rightarrow !Y$  observed.  $Y$  is hypothesized to be suppressed by  $X_2$  and  $X_3$ . (e)  $X_0, X_2 \rightarrow !Y$  observed.  $X_3$ , seen unnecessary for suppression of  $Y$ , refined. Correct structure learned and is stable from now on.

## A. Appendix

### A.1. Figures and algorithms detailing original design of Modelleyen

This section provides some brief background information in Modelleyen. All figures and papers are taken from (Erden & Faltings, 2025a), the reader is referred to there for full context and details.

Figure 6 illustrates the formation of the sources composition of a CSV, and Fig. 7 illustrates the formation of upstream conditioning pathways. Algorithm 2 gives an overview of the per-step learning loop in Modelleyen, and Alg. 3 provides a complete view into the per-step state-computation operations of a CSV, which is the focus of learning in the algorithm. This learning flow is kept intact in our design as well, with the exception of the changes listed in Section 3.2.3.

---

**Algorithm 2** From (Erden & Faltings, 2025a). Pseudocode of the main Modelleyen adaptation loop; formed of state computations followed by CSV generation for unexplained SVs.

---

**Parameter:**  $N$  Set of all target nodes

**Function** *ProcessEnvironmentStep*(observations)

- 1:  $BSVStates \leftarrow observations$
  - 2: *ComputeDSVStates*() {Computes DSV states by BSV events}
  - 3: **for**  $level \in reverse(ComputationLevels)$  **do**
  - 4:   **for**  $CSV \in SVs_n(level)$  **do**
  - 5:     *ComputeState*( $CSV$ )
  - 6:   **end for**
  - 7: **end for**
  - 8:  $UnexplainedSVs \leftarrow [SV : SV.state = 1 \text{ and } NoConditionerActive(SV)]$
  - 9:  $sources \leftarrow [SV : SV \text{ in } [BSVs, DSVs] \text{ and } SV.state = 1 \text{ and } isEligible(SV)]$
  - 10:  $NewCSV = CreateCSV(sources, [SV : SV \text{ in } UnexplainedSVs \text{ and } TargetEligible(SV)])$
  - 11: *ModelRefinement*() {Removes CSVs with no source or target}
-



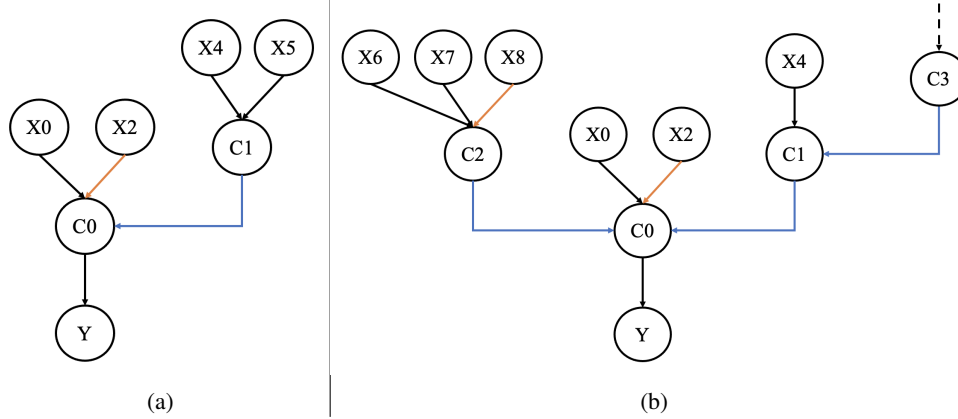


Figure 7. From (Erden & Faltings, 2025a). Example of upstream conditioning, continuing from Figure 6. Assume that the unconditionality flag of  $C0$  is set following an observation that  $(X0, !X2)$  did not result in its activation (see main text). (a)  $X0, !X2, X4, X5 \rightarrow Y$  observed.  $C0$  is observed to be active, since  $X0, !X2$  led to  $Y$ . A new CSV  $C1$  is formed & conditions  $C0$ . Note that  $(X4, X5)$  alone will not predict activation of  $C0$  if  $C0$ 's sources are not also active. (b) New conditioners are also subject to the CSV processes: Here, the source  $X5$  of  $C1$  has been refined, and new conditioners  $C2$  and  $C3$  are formed. Multiple conditioners represent alternative paths: In this case,  $C0$  is expected to be active when sources of either  $C1$  or  $C2$  is active. Any logical function can hence be incorporated in a conditioning pathway in a minimal and ongoing manner without destroying past knowledge.

## A.2. Additional illustrations

Figure 8 presents some additional learned representations in the runs during our experiments presented in the main text.

## A.3. Experimental details

**Sample sizes:** We use  $N_{sample} = 20, 10, 5$  and test set size of 50, 20, 10 samples per class for experiments with  $N_C = 3, 5, 10$  respectively. Reported results are averages of 10 runs for  $N_C = 3$  and 5 runs for  $N_C = 5$ . Population size for generating assignments was chosen as 10 for both learning and prediction.

**MNR settings:** For MNR, we choose refinement threshold  $T_{ref} = 0.05$ , significance threshold  $T_{sign} = 0.05$ .  $\epsilon$  for polygonal approximation is  $0.01L$  where  $L$  is the arc length of contour being approximated.

**Neural network settings:** Our fully connected neural network architecture is of 2 hidden layers with 128 neurons each, while the CNN architecture has a pair of convolutional (32 filters with  $3 \times 3$  kernels) and max-pooling (with pool size  $2 \times 2$ ) layer, repeated twice sequentially, followed by a dense layer of 128 neurons. All NNs use ReLU activation in hidden layers and softmax in output. We use a maximum of 100 epochs and an early stopping patience of 10 epochs. All remaining settings are Keras defaults.

**Prediction in MNR** To predict targets for a given observed SPN, we follow this procedure: First, we attempt to find an assignment (as described in 3.2.2) that *satisfies* the source SPN of the CSV. If no assignment is found, the CSV is considered inactive. If an assignment is found, we compute the activation probability of the CSV. If the CSV is unconditional (no positive/negative conditioners), the probability is  $p = P(I(T)|SS(C))$ , tracked over the learning process. If the CSV is conditional, the probability is  $p = (1 - p^{max-}) \times p^{max+}$ , where  $p^{max-}$  and  $p^{max+}$  are the maximum activation probabilities of negative and positive conditioners, respectively. Intuitively, this approach prioritizes the most-upstream representations (most closely matching the observed SPN) when calculating the final probability, resolving conflicts between activating and suppressing pathways by multiplying their probabilities.

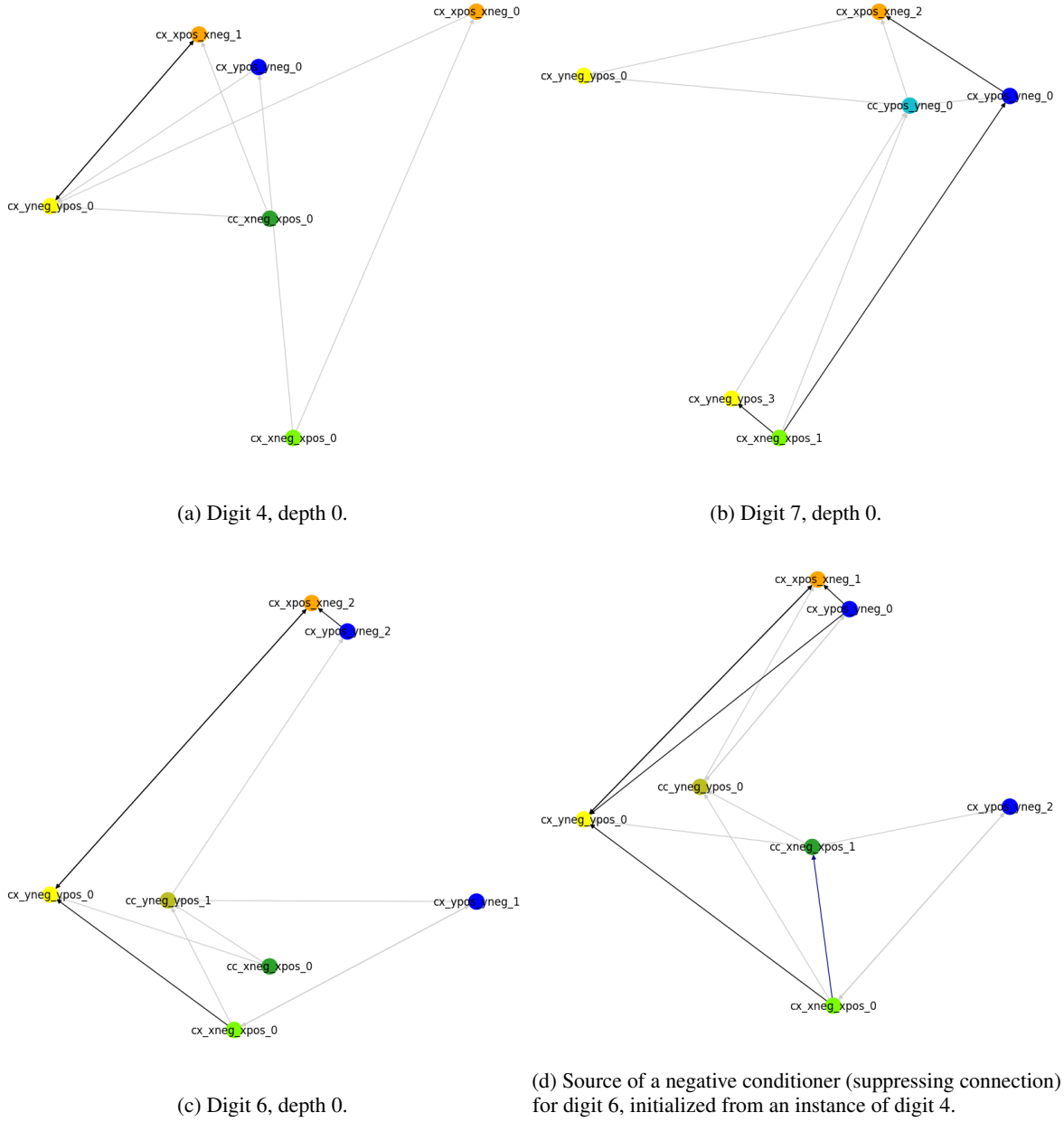


Figure 8. Additional examples of representations of digits learned by MNR.

---

**Algorithm 3** From (Erden & Faltings, 2025a). Pseudocode for CSV state computation.

---

**Function** *ComputeState(CSV)*

```

1: if AnySourceActive() then
2:   SeparateActiveInactiveTargets() {Creates two CSVs from current one with active and inactive targets in either
   of them}
3:   if AnyTargetObserved() then
4:     State = 1
5:     PosSources  $\leftarrow$  [source : source in PosSources and source.state = 1]
6:     NegSources  $\leftarrow$  [source : source in NegSources and source.state! = 1]
7:   else if AnyTargetInactive() then
8:     if not(AllSourcesActive()) then
9:       State = 1
10:    else
11:      if AnyNegativeSourceActive() then
12:        State = 0
13:        NegSources  $\leftarrow$  [source : source in NegSources and source.State = 1]
14:      else
15:        State = -1 {No negative source active to explain inactivity of targets}
16:      end if
17:    end if
18:  end if
19: else
20:   State = 0 {Unobserved if targets are not observed}
21: end if
22: if State = -1 then
23:   if NegativeConnectionsFormed then
24:     FormNegativeConnections()
25:   else
26:     unconditionality = "isConditional" {-1 for }
27:   end if
28: end if

```

---